Bound and resonant electron states in quantum dots: The optical spectrum

R. Buczko
Institute of Physics, Polish Academy of Sciences, aleja Lotników 32/46, 02-668 Warszawa, Poland

F. Bassani
Scuola Normale Superiore, Piazza dei Cavalieri, I-56100 Pisa, Italy

(Received 21 August 1995)

The energy spectrum and the wave functions of an electron in a quantum dot (QD) are computed using the effective-mass approximation. The case of a shallow, hydrogenlike center in a quantum dot is also considered. We use the spherical shape approximation in the belief that the basic results are more sensitive to the dimensions than to the shape of the confining potential. The wave functions for the discrete bound states and for the continuum states are obtained in a closed form. We show that resonances of the Breit-Wigner type occur in the continuum, due to the local potential of the microstructures. The lifetimes of the resonant states are computed and their impact on the optical properties of the QD material is discussed. As an example, we give detailed results for the GaAs/$Ga_{1-x}Al_x$As QD, where the basic properties (band mismatch, effective masses, dielectric constants) are well known. We find that the optical excitation spectrum, with or without the impurity center, depends dramatically on the dot radius. [S0163-1829(96)01127-7]

I. INTRODUCTION

Recent improvements in microstructure technology have made it possible to prepare quantum dots (QD's) characterized by confining potentials in all directions;[1] for instance, QD's prepared by using molecular-beam epitaxy (MBE) techniques with $Ga_{1-x}Al_x$As alloys[2] or semiconductors of spherical shape in glasslike materials.[3,4]

The relevance of such materials, both for the fundamental study of electronic states and for technological applications, is evident, considering that zero dimensionality in translational symmetry may produce discrete levels whose energies can be varied just by changing the size of the QD. These levels act as traps for electrons and holes, which can be introduced into the crystal either by doping with donor or acceptor impurities or by the absorption of electromagnetic radiation in the interband transition region. In addition to bound states, the local potential of the microstructure can also produce resonant states in the continuum, which may have considerable influence on the properties of QD materials.

The electron bound states of an electron in a quantum dot have been calculated for various types of confining potentials, such as steplike barriers,[5,6] parabolic potentials which produce equally spaced levels,[7] and potentials due to strain interactions.[8] Various QD shapes have been considered,[9,10] though the spherical shape has been preferred in the theoretical approach because of its calculational simplicity. Also the discrete states of a hydrogenlike impurity located inside the dot have been computed in the case of infinite[11] and finite[12,13] potential barriers. The dependence of the energy spectrum on the donor position has also been discussed.[14,15]

In this paper we study the electron states of a QD within the spherical shape approximation, on the assumption that the basic results are sensitive to the dimension, but not to the shape, of the confining potential. We are interested not only in discrete levels, but also in the states of the continuum, and particularly in resonant states of the type introduced by Breit and Wigner[16,17] in nuclear physics and by Fano[18] in atomic and condensed matter physics. We give a recipe on how to compute bound states and free states in the continuum using the envelope function approach and a steplike confining potential, and show how they depend on the radius of the quantum dot. We apply the standard scattering theory to compute the wave functions in the continuum and to identify the resonances. The lifetimes of some of the resonant states are long enough to qualify them as Breit-Wigner resonances.

Bound states influence the statistical distribution of electrons in the conduction band, since they compete with impurity states as local traps. We study the infrared absorption spectrum of electrons in the QD's and show that strong peaks arise due to transitions to discrete and resonant levels.

We consider also the case when the QD contains an impurity or has trapped either an electron or a hole, so that a Coulomb-like potential is superimposed on the confining potential of the neutral zero-dimensional structure. When this potential is repulsive outside the dot, the total potential is very similar to the nuclear potential considered by Breit and Wigner for the α decay.[17] For this reason we use the notion of Breit-Wigner resonances.[16]

In Sec. II we apply the envelope function method to compute bound and continuum states for an electron in a QD, without and with an additional electric charge. We show how to find the resonances and their lifetimes and how to calculate the oscillator strengths for optical transitions from the ground state. In Sec. III we present the detailed results for a GaAs/$Ga_{1-x}Al_x$As QD, where the basic parameters (band mismatch, effective masses, dielectric constants) are well known. Conclusions are given in Sec. IV.

II. THEORY

We compute the electron trapping states in a spherical quantum dot with radius R in three cases: without an internal

charge and with a positive or negative Coulomb charge at the center of the dot. We use the effective-mass approximation assuming that the Bloch functions at the minima of the conduction band are the same outside and inside the dot, which is a typical assumption for materials like GaAs/$Ga_{1-x}Al_xAs$. We take the conduction band to be parabolic in $\mathbf{k}$ space. In our treatment we neglect any effect of the electron on its own potential. In some calculations a term accounting for different polarizabilities of the material inside the QD and outside the barrier has been calculated,[17,20–22] but we choose not to take this effect into account because only a self-consistent calculation which takes into account the dependence of the polarizability on the wave function of the electron would give an improvement. In addition, for the sake of convenience, we have not considered the image charge potential of the impurity; this is a minor effect which can modify only the numerical details. With the above approximations, the calculation can then be performed in the framework of standard quantum mechanics scattering theory.[23]

Let the effective masses of the electron be m_1 inside the dot and m_2 outside the dot and the dielectric constants be ε_1 and ε_2, respectively. We choose as units of energy and length the effective Rydberg $\mathrm{Ry}^*=m_1e^4/2\hbar^2\varepsilon_1^2$ and the effective Bohr radius $a^*=\hbar^2\varepsilon_1/m_1e^2$, defined with the parameters of the material inside the dot. Due to the spherical symmetry, the envelope wave functions have the general form of

$$\Psi_{E,l,m}(\mathbf{r})=F_{E,l}(r)Y_{l,m}(\vartheta,\varphi). \tag{1}$$

For the kinetic part of the Hamiltonian we adopt the widely used Hermitian form:

$$-\nabla\frac{1}{\mu(r)}\nabla, \tag{2}$$

so that the radial effective-mass equation reads

$$\left[-\frac{1}{r^2}\frac{d}{dr}\frac{r^2}{\mu(r)}\frac{d}{dr}+\frac{l(l+1)}{\mu(r)r^2}+U(r)-\frac{2Z}{\varepsilon(r)r}\right]F_{E,l}(r)=E_lF_{E,l}(r), \tag{3}$$

where

$$\mu(r)=\begin{cases}1, & r<R\\ \dfrac{m_2}{m_1}, & r>R,\end{cases}\qquad \varepsilon(r)=\begin{cases}1, & r<R\\ \dfrac{\varepsilon_2}{\varepsilon_1}, & r>R,\end{cases} \tag{4}$$

and Z is the charge of the impurity located in the center of the dot. U is the confining potential of the dot:

$$U(r)=\begin{cases}-U_0, & r<R\\ 0, & r>R.\end{cases} \tag{5}$$

The Hermiticity of the Hamiltonian forces the following boundary conditions:

$$\lim_{\varepsilon\to0}F_{E,l}(R-\varepsilon)=F_{E,l}(R+\varepsilon),$$

$$\lim_{\varepsilon\to0}F'_{E,l}(R-\varepsilon)=\frac{1}{\mu}F'_{E,l}(R+\varepsilon). \tag{6}$$

In addition $F_{E,l}$ must be regular for $r=0$. For the energies of the discrete spectrum ($E<0$) the functions $F_{E,l}(r)$ must be integrable, and we normalize them to 1. In the continuum spectrum ($E>0$) we normalize our solutions to $\delta(E'-E)$ and express them in the outside region as the sum of incoming F^- and outgoing F^+ spherical waves. For a given energy Eq. (3) has analytical solutions, which we denote as follows:

$$F_{E,l}(r)=AF^{\mathrm{in}}_{E,l}(r)\quad \text{for } r<R,$$

$$F_{E,l}(r)=BF^{\mathrm{out}}_{E,l}(r)\quad \text{for } r\geqslant R \text{ and } E<0, \tag{7}$$

$$F_{E,l}(r)=F^-_{E,l}(r)+e^{2i\delta_l}F^+_{E,l}(r)\quad \text{for } r\geqslant R \text{ and } E\geqslant0.$$

The constants A and B are given by boundary and normalization conditions in the case of $E<0$; A and the phase shift δ_l are given by boundary conditions in the case $E\geqslant0$. The inside wave functions are

$$F^{\mathrm{in}}_{E,l}(r)=j_l(kr)\quad \text{for } Z=0,$$

$$F^{\mathrm{in}}_{E,l}(r)=(2kr)^le^{-ikr}{}_1F_1\left(l+1+i\frac{Z}{k},2l+2,2ikr\right)\quad \text{for } Z\neq0, \tag{8}$$

where $k=\sqrt{E+U_0}$, j is the spherical Bessel function, and ${}_1F_1$ is the Kummer function.[24]

It is easy to find the wave functions outside the dot when $m_2=m_1$ and $\varepsilon_2=\varepsilon_1$. In this case we denote the appropriate radial wave functions by $\tilde{F}^{\mathrm{out}}$ and $\tilde{F}^{\pm}$. For $Z=0$ we obtain

$$\left.\begin{aligned}\tilde{F}^{\mathrm{out}}_{E,l}(r)&=i^lh^{(1)}_l(i\chi r)\\ \tilde{F}^{+}_{E,l}(r)&=\frac{1}{2}\left(\frac{k}{\pi}\right)^{1/2}h^{(1)}_l(kr)\\ \tilde{F}^{-}_{E,l}(r)&=\frac{1}{2}\left(\frac{k}{\pi}\right)^{1/2}h^{(2)}_l(kr)\end{aligned}\right\}\quad \text{for } Z=0, \tag{9}$$

where $\chi=\sqrt{-E}$ ($E<0$), $k=\sqrt{E}$ ($E\geqslant0$), and $h^{(1,2)}_l$ are the spherical Hankel functions. For $Z\neq0$ we obtain the following expressions in terms of the Kummer functions of type U:

$$\tilde{F}^{\mathrm{out}}_{E,l}(r)=(2\chi r)^le^{-\chi r}U\left(l+1-\frac{Z}{\chi},2l+2,2\chi r\right),$$

$$\tilde{F}^{\pm}_{E,l}(r)=-(-2kr)^l2\left(\frac{k}{\pi}\right)^{1/2}e^{Z\pi/2k}e^{\pm i\sigma_l}e^{\pm ikr}\times U\left(l+1-i\frac{Z}{k},2l+2,\pm2ikr\right)\quad \text{for } Z\neq0. \tag{10}$$

Here $\chi=\sqrt{-E}$ $(E<0)$, $k=\sqrt{E}$ $(E\geqslant 0)$, and σ_l is the Coulomb phase shift:

$$\sigma_l=\arg\left[\Gamma\left(l+1-i\frac{Z}{k}\right)\right], \tag{11}$$

where Γ indicates the Euler function.

For $m_2\neq m_1$ and (or) $\varepsilon_2\neq\varepsilon_1$ the effective Rydbergs and the effective Bohr radii are not the same in both materials. Still, the solutions in this case can be obtained from those given in Eqs. (9) and (10) by a simple scaling procedure:

$$|F^{\rm out}_{E,l}(r)|^2 r^2 dr=|\widetilde{F}^{\rm out}_{E',l}(r')|^2 r'^2 dr',$$

and

$$|F^{\pm}_{E,l}(r)|^2 r^2 dr dE=|\widetilde{F}^{\pm}_{E',l}(r')|^2 r'^2 dr' dE', \tag{12}$$

where $ra_1^*=r'a_2^*$, $E\times{\rm Ry}_1^*=E'\times{\rm Ry}_2^*$, and the indices refer to inner (1) and outer (2) Bohr radii and Rydberg units. The above conditions express the fact that the probability of finding the electron in a given spatial area (or spatial and energetic area in the case of the continuum spectrum) does not depend on the adopted units. We obtain from (12)

$$F^{\rm out}_{E,l}(r)=\gamma^{3/2}\widetilde{F}^{\rm out}_{\beta E,l}(\gamma r),$$

$$F^{\pm}_{E,l}(r)=\gamma^{3/2}\beta^{1/2}\widetilde{F}^{\pm}_{\beta E,l}(\gamma r), \tag{13}$$

where $\gamma=a_1^*/a_2^*=\varepsilon_1 m_2^*/\varepsilon_2 m_1^*$ and $\beta={\rm Ry}_1^*/{\rm Ry}_2^*=\varepsilon_2^2 m_1^*/\varepsilon_1^2 m_2^*$. The scaling factor $\gamma^{3/2}$ of the $F^{\rm out}$ function can be included into the B constant of Eq. (7), but we must conserve the value $\gamma^{3/2}\beta^{1/2}$ in the expressions for the $F^{\pm}$ functions, in order to preserve normalization in the energy space.

The boundary conditions (6) give discrete levels in the $E<0$ energy region. We denote the discrete energies and the radial wave functions by $E_{n,l}$ and $F_{n,l}$, respectively.

In the region $E>0$ the asymptotic forms of the radial wave functions of the continuum spectrum are

$$F_{E,l}(r)\underset{r-\infty}{\rightarrow}\frac{e^{i\delta_l}}{\sqrt{\pi\sqrt{\beta E}}}\frac{\sin(kr+\delta_l-l\pi/2)}{r}\quad\text{for } Z=0,$$

$$F_{E,l}(r)\underset{r-\infty}{\rightarrow}\frac{e^{i\delta_l}}{\sqrt{\pi\sqrt{\beta E}}}\frac{\sin[\sqrt{\beta E}r-(Z/\sqrt{\beta E})\ln(2kr)+\sigma_l+\delta_l-l\pi/2]}{r}\quad\text{for } Z\neq 0, \tag{14}$$

where now $k=\sqrt{m_2/m_1}E$ and $\sigma_1=\arg[\Gamma(l+1-iZ/\sqrt{\beta E})]$. The phase shift δ_l can be expressed as a sum of two factors, $\delta_l=\xi_l+\rho_l$. The first factor, ξ_l, describes the phase shift resulting from the hard-sphere scattering:

$$e^{2i\xi_l}=-\frac{F^-_{E,l}(R)}{F^+_{E,l}(R)}, \tag{15}$$

while the second term, ρ_l, depends on the potential inside the dot. In the vicinity of the energies E_r, which are given by

$$\rho_l(E_r)=(2n+1)\frac{\pi}{2},\quad n=0,1,2,\ldots, \tag{16}$$

the phase shift ρ_l can be expressed through

$$e^{2i\rho_l(E)}=\frac{E-E_r-\frac{1}{2}i\Gamma}{E-E_r+\frac{1}{2}i\Gamma}, \tag{17}$$

with

$$\Gamma=2\left(\frac{d\rho_l}{dE}\bigg|_{E=E_r}\right)^{-1}. \tag{18}$$

The resonances $(E_r-i\Gamma/2)$ are then the poles of the scattering matrix $S_l(E)=e^{2i\delta_l(E)}$ in the complex energy plane. They are of the Breit-Wigner type[23] when the value of $\Gamma/2$ is small in comparison with $(d\rho_l/dE)^{-1}$ away from E_r. Resonances of this type occur in many fields of physics; in optics they are known as Fabry-Pérot resonances for interference of electromagnetic waves in slab-shaped substances and as Mie resonances for scattering on spherical particles.[25]

An approximate rule to decide when there exist well-defined resonances can be found by expressing the radial functions in the form $F(r)=f(r)/r$, so that for $f(r)$ we have a one-dimensional Schrödinger equation:

$$\left(-\frac{d}{dr}\frac{1}{\mu(r)}\frac{d}{dr}+V_{\rm ef}(l,r)\right)f_{E,l}(r)=E_l f_{E,l}(r),$$

where

$$V_{\rm ef}(l,r)=U(r)+\frac{l(l+1)}{\mu(r)r}-\frac{2Z}{\varepsilon(r)}\quad\text{if } r>0 \tag{19}$$

and

$$f_{E,l}(0)=0.$$

If $V_{\rm ef}(l,R)>0$ there is an energy barrier which produces narrow resonant states in the continuum spectrum. We distinguish three cases depending on the presence of the Coulomb-like potential.

(i) $Z=0$ (no impurity); the barrier is given by the centrifugal term and exists only for $l>0$.

(ii) $Z>0$ (donor impurity); the barrier exists only if $l>0$ and $R<[l(l+1)/2Z](\varepsilon_2 m_1^*/\varepsilon_1 m_2^*)$.

(iii) $Z<0$ (compensated acceptor); the barrier always exists, even for $l=0$.

The optical (intersubband) transitions between the ground and the excited states can be studied based on the computed energies and wave functions. Since the ground state has s symmetry ($l=0$), only p-type states ($l=1$) need to be considered within the standard dipole approximation. The oscillator strength for an optical transition from the ground state $|0\rangle$ to a state $|\nu\rangle$ is given by

$$f_{0\nu}=\frac{C}{\Delta E}\left|\left\langle \nu\left|\frac{\mathbf{a}(\mathbf{r})}{m(r)}\cdot\nabla+\nabla\cdot\frac{\mathbf{a}(\mathbf{r})}{m(r)}\right|0\right\rangle\right|^2, \tag{20}$$

where C is an appropriate constant required when using the effective-mass approximation and $\mathbf{a}$ is the unit vector in the polarization direction of the perturbing electric field, since we apply the approximation $\varepsilon_1=\varepsilon_2$ in the description of the incident radiation. Choosing the polarization in the z direction and using the commutation relation $[H,z]=-(1/\mu(r))\nabla_z-\nabla_z 1/\mu(r)$ we obtain

$$f_{0\nu}=C\Delta E|\langle \nu|z|0\rangle|^2. \tag{21}$$

The value of the constant C can be obtained by requiring that the Thomas-Reiche-Kuhn sum rule

$$\sum_n f_{0n}+\int_0^\infty f_{0E}dE=1 \tag{22}$$

should apply, and turns out to be[26]

$$C=\left\langle 0\left|\frac{1}{\mu(r)}\right|0\right\rangle^{-1}. \tag{23}$$

We recall that the matrix element $\langle 0|z|\nu\rangle$ is not equal to zero only for such final states $\Psi_{\nu,1,0}$ for which $l=1,m=0$:

$$\langle 0|z|\nu\rangle=\int \Psi_{0,0,0}(\mathbf{r})z\Psi_{\nu,1,0}(\mathbf{r})d^3r$$

$$=\frac{1}{3}\int_0^\infty F_{0,0}(r)F_{\nu,1}(r)r^3dr. \tag{24}$$

III. RESULTS FOR GaAs/$Ga_{1-x}Al_xAs$

Rather than discussing the general properties of electron levels in QD's and related optical effects, we chose to carry out detailed calculations for the case of a material whose two-dimensional and one-dimensional nanostructures have been extensively investigated. Electron states in spherically shaped GaAs/$Ga_{1-x}Al_xAs$ QD's have been studied in the approximation of infinite potential barriers.[5,11] In the case of finite barriers only the bound states have been considered.[6,12,15,27]

The optical properties of electrons trapped inside quantum dots by the confining potential and by the Coulomb potential of the impurity strongly depend on the aluminum content in the barrier and on the dot radius. For quantum dots the scattering resonant states become of relevance, as we will show in detail. We choose the matrix composition to be 20% of Al, so that all the parameters needed for the calculations are those of Table I.

We first consider the case of a QD without an impurity,

TABLE I. Material parameters for GaAs/$Ga_{0.8}Al_{0.2}As$.

$m_1=0.0657m_0$ $m_2=0.0750m_0$	Ref. 28
$\varepsilon_1=12.4$ $\varepsilon_2=11.84$	Ref. 29
$a^*=a_1^*=99.9$ Å	
$\mathrm{Ry}^*=\mathrm{Ry}_1^*=5.81$ meV	
$U_0=0.178$ eV $=30.6$ Ry*	Ref. 30

and report in Fig. 1 the energies of bound and resonant states with $l\leq 3$ versus inverse dot radius. It can be seen that bound states exist only for $R>27$ Å. This is very close to the condition $R>\pi(/2\sqrt{U_0})$, which is obtained assuming that the radial wave function vanishes at the boundary. As we increase the size of the QD we observe that the binding energy of the ground state increases and other bound states appear, starting from $R=55$ Å (the second one being the $l=1$ state, the third $l=2$, then another $l=0$, and so on). In addition to bound states, we find resonances in the continuum. Such resonances are of the Breit-Wigner type when the broadening is sufficiently small. We find that a convenient criterion for such a classification is the requirement for the resonant energy to be lower than the peak of the potential barrier $V_{\mathrm{ef}}(R)$ as given by expression (19). The states fulfilling such a condition are indicated by the solid line in Fig. 1. It turns out that the Breit-Wigner resonances are narrower and occur in a larger positive-energy region as the value of l increases. We observe that there is a correspondence between bound and resonant states. As the radius of the QD decreases the bound states continuously transform into resonant states and a critical value of the radius for this transformation can be found for each state.

We have computed the optical transition probabilities from the ground state to all excited states. In Fig. 2 we show the oscillator strengths as a function of energy for three chosen values of the dot radius. While the values in the entire spatial region always satisfy the sum rule (21), the peaks and line shapes strongly depend on the dot size. For the three cases reported in Fig. 2, most of the oscillator strength is taken by the first transition ($f_{0,1}>90\%$) when the dot size is sufficiently large to have more than one bound state. As the radius decreases, we observe that a resonant transition appears above the ionization energy. Finally, for very small radii most of the oscillator strength is taken up by the first resonance.

We have found that the results presented in Figs. 1 and 2 can be easily scaled to the case of different Al compositions in the barrier. The impact of the composition on the value of U_0 of the potential barrier is much greater than the influence on the effective mass. This condition allows us to use the scaling procedure presented in Appendix A. We have found that the scaling formulas (A4) and (A5) reproduce the energies and the oscillator strengths almost exactly for various potential depths.

We have also computed bound and resonant states, as well as oscillator strengths for transitions from the ground state, for a quantum dot containing a compensated acceptor impurity ($Z=-1$) at the center. The results are similar to those obtained for an empty QD, and are displayed in Figs. 3 and 4. It can be seen that in this case the widths of the resonant states are narrower. The narrow resonant states exist

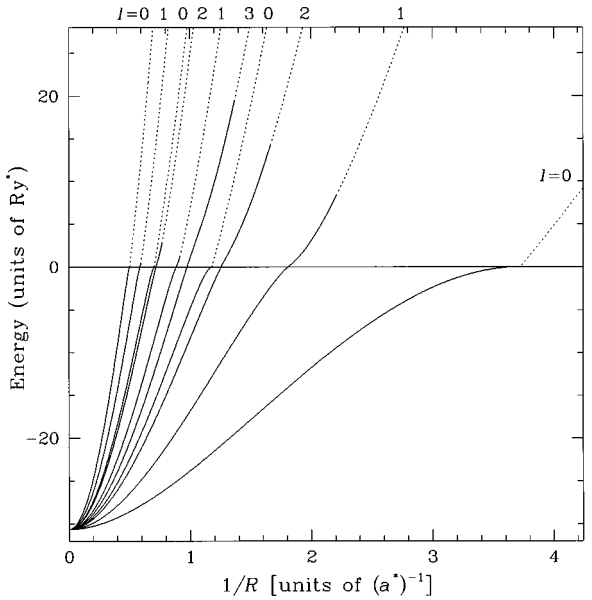

FIG. 1. Energies of the electron states in an empty GaAs/$Ga_{0.8}Al_{0.2}As$ spherical QD as a function of the inverse of the dot's radius. The lowest states with $l=0$, 1, 2, and 3 are presented. The energy values $E>0$ correspond to resonant states in the continuum. Breit-Wigner resonances with energies smaller than the $V_{eq}(l,R)$ barrier height are denoted by solid lines.

even for $l=0$. In general the role of resonant states in the optical spectrum is increased, their peaks being narrower and characterized by larger oscillator strength densities.

The case of a donor impurity in a QD ($Z=+1$) is qualitatively different, because an infinite set of bound states is always present, irrespective of the value of R. Still, the confining potential produces two important effects, similar to those presented above. The first is the increase of the binding energies with increasing radius, where in our case the binding energy is defined relative to the ionization limit. The ground state, for instance, changes from Ry_2^* for a very small dot radius to $U_0+Ry_1^*$ for very large dots, where small and large refer to size as compared with the Bohr effective radius. A similar change is observed for the excited-state energies (small and large dots refer in this case to the mean

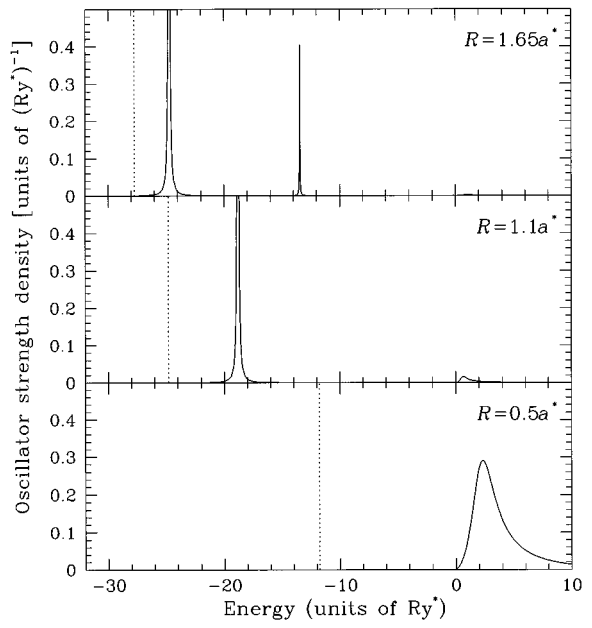

FIG. 2. Computed spectra of the transitions from the ground state ($l=0$) to the excited p-type ($l=1$) bound and continuum states of an empty GaAs/$Ga_{0.8}Al_{0.2}As$ spherical QD. Results are presented for three different dot radii. The finite widths of the discrete level transitions are obtained by adopting a 0.04 Ry* wide Lorentzian line shape. The energies refer to the ionization limit and the dotted vertical lines denote the ground-state positions.

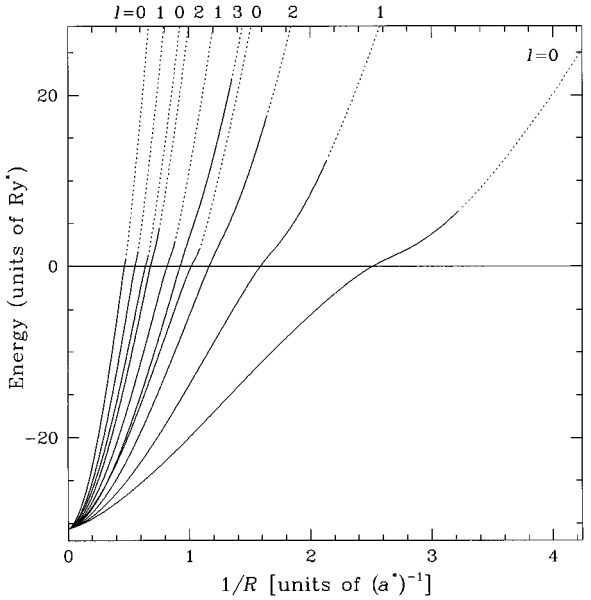

FIG. 3. The same as in Fig. 1, but for a compensated acceptor impurity ($Z=-1$) at the center of a GaAs/$Ga_{0.8}Al_{0.2}As$ spherical QD.

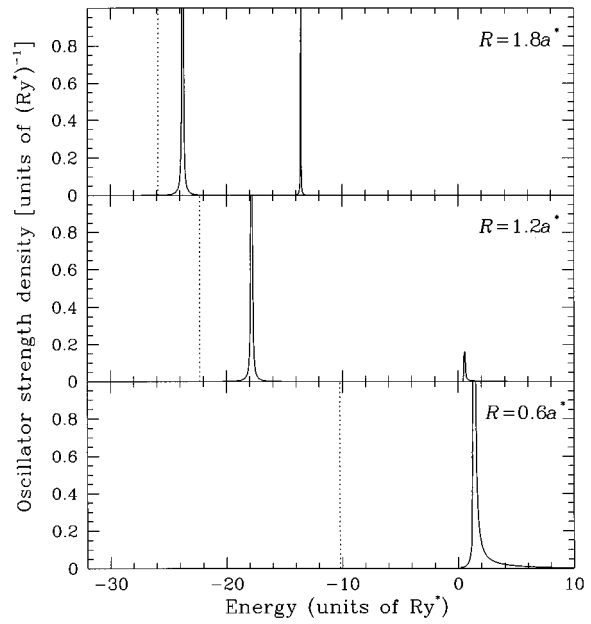

FIG. 4. The same as in Fig. 2, but for a compensated acceptor ($Z=-1$) in the center of the dot. Results are presented for three values of the QD radius.

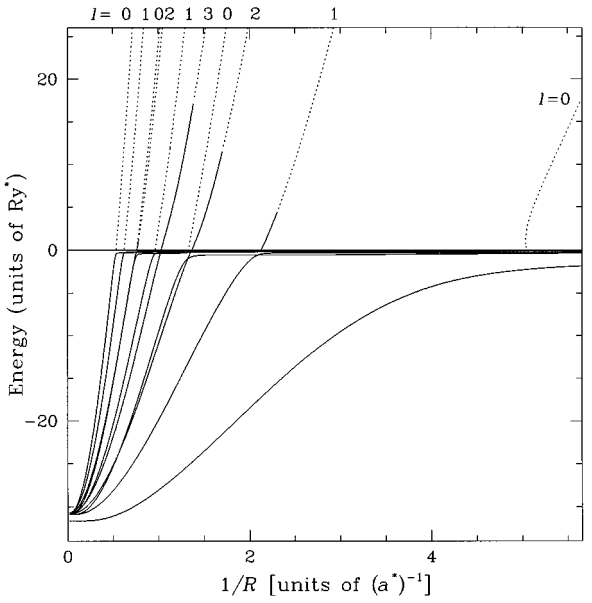

FIG. 5. The same as in Fig. 1, but for a donor impurity ($Z=1$) at the center of a GaAs/$Ga_{0.8}Al_{0.2}As$ spherical QD. The presented states correspond to the $n\leq 4$ hydrogenlike bound states in the bulk.

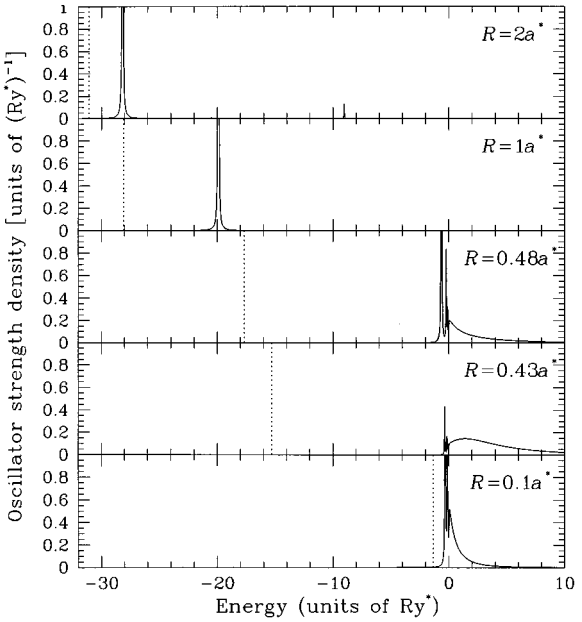

FIG. 7. The same as in Fig. 2, but for a shallow donor impurity ($Z=1$) in the center of the dot. Results are presented for five values of the QD radius.

radius). The second effect is the appearance of resonances analogous to those for the empty QD, which do not appear in the case of a purely Coulombic potential. They are much weaker and satisfy our criterion of Breit-Wigner resonances only in a small range of R values. The resonant states appear when the wave functions of the corresponding bound states are predominantly outside the well. The above discussed results are summarized in Fig. 5.

In the case of p states, the appearance of resonances affects the optical spectra significantly. The oscillator strength is transferred to the continuum, while the corresponding bound-state transition loses almost all its intensity. This effect is shown quite clearly in Fig. 6, where the oscillator strength for the transition from the ground state to the first p state is compared with that for the transition to the continuum. It can be seen that, with decreasing dot radius, the oscillator strength for the transition to the first p bound state increases initially from the hydrogen value of 0.42 to almost 1 when R drops to about $\frac{1}{2}a^*$, then it falls down to about 0

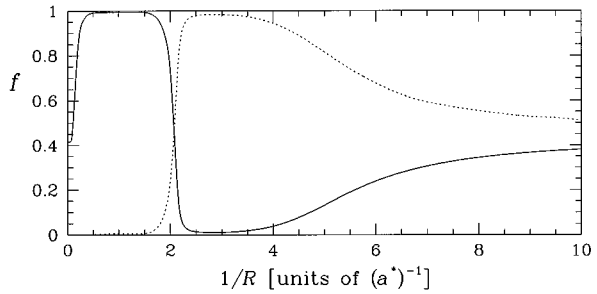

FIG. 6. Computed oscillator strengths for transitions from the ground to the first $l=1$ state (solid line) and to the continuum (dashed line) for the case of a shallow donor inside the dot as a function of inverse dot radius.

when the resonance appears, and increases again to the asymptotic value of 0.42 when the wave function of the ground state extends outside the confining region of the QD.

The existence of resonant states, in this case, changes the excitation spectrum dramatically. In Fig. 7 we present the calculated spectra for five different dot radii. For $R=2a^*$ one strong absorption peak is visible while the second one is orders of magnitude weaker. For $R=a^*$ only one strong absorption peak occurs, since the second p state has lost all its oscillator strength. For $R=0.48a^*$ both discrete and continuum transitions are observed, with one peak corresponding to the resonant state. The appearance of a resonant transition is well exemplified for $R=0.43a^*$, where a very broad resonance with a peak at 1.5 Ry* in the continuum can be seen. When the value of R reaches $0.1a^*$, the hydrogenlike spectrum is recovered because the notion of a quantum dot is no longer valid. The confining potential corresponds now to a central-cell correction to the impurity potential.

In the case of an impurity inside the dot ($Z\neq 0$) the potential cannot be scaled, in general, with the dot radius. We have found, however, that the scaling formulas (A4) and (A5) can be adopted, but only for dot radii for which the confinement energy is greater than the Coulombic one.

In Table II we compare the widths of the resonant states obtained in the three ($Z=0,-1,1$) cases discussed above. In general, the attractive potential ($Z=1$) makes the resonances very wide; what makes them narrow is the additional repulsive potential ($Z=-1$). We can also observe that the widths diminish as the value of l increases.

A further comment is in order when more electrons are considered in the confining potential of the quantum dot. Neglecting the effects of exchange and correlation, which have to be taken into account, the situation can be reduced to the case of an electron in the confining potential of the QD subjected additionally to the Coulomb repulsive potential of the other electron trapped inside the QD. The resonances will

TABLE II. Widths Γ of the resonant states (in effective Rydberg units), at the energy of $E=1$ Ry*. R is the dot radius for which the resonance appears, given in units of effective Bohr radius.

	$Z=0$		$Z=-1$		$Z=1$	
l	R	Γ	R	Γ	R	Γ
0	0.26	14.9	0.37	0.14	0.19	
	0.83	4.48	0.94	0.32	0.74	11.80
	1.39	2.67	1.51	0.50	1.28	5.11
	1.95	1.90	2.07	0.63	1.83	3.14
1	0.53	0.83	0.61	0.049	0.46	6.74
	1.10	1.48	1.19	0.15	1.02	4.92
	1.66	1.54	1.75	0.28	1.57	3.21
2	0.77	0.12	0.83	0.011	0.71	0.80
	1.34	0.38	1.43	0.044	1.28	1.71
3	1.00	0.03	1.05	0.021	0.95	0.11

be more pronounced the larger the number of trapped electrons.

IV. CONCLUSIONS

The main results obtained in the present work can be summarized as follows.

We have given analytical expressions for bound states in QD's, both empty and containing either a donor or an acceptor impurity. We have shown that resonant states appear in the continuum, and their positions and energy widths depend on the well size and on the values of the confining potentials.

The optical excitation spectrum of an electron for a given barrier potential strongly depends on the size of the QD and it shows strong resonance peaks in the continuum when the radius of the QD is smaller than the Bohr radius. When decreasing the radius of a dot containing a donor impurity, we proceed from a hydrogenlike spectrum to a situation where almost all the absorption is in the continuum, with a broad peak at the resonance energy.

The results presented here for a GaAs/$Ga_{1-x}Al_xAs$ dot can easily be extended to other materials; the critical values of the potential barrier and of the radii will change according to the values of the material parameters. The case when more electrons are considered is expected to produce an enhancement of the resonance transition due to the repulsive long-range Coulomb potential.

ACKNOWLEDGMENTS

The authors wish to acknowledge support from the Polish Scientific Committee, Grant No. 2 23469203 and from the Italian Research Council (CNR), Grant No. 95.01910.ST74. One of the authors (R.B.) wishes to thank Scuola Normale Superiore for its hospitality when part of this work was carried out. We are also indebted to Pawel Janiszewski and Giuseppe La Rocca for useful suggestions.

APPENDIX: SCALING WITH THE POTENTIAL DEPTH

Let us consider the case of an empty dot [$Z=0$ in Eq. (3)]. Assuming that for a given potential depth U_0 we know the solutions of Eq. (3) and their dependence on R, we want to find the solutions for a potential $\beta U_R(\mathbf{r})$, where β is a positive constant. We assume that the ratio of the effective masses in (4) does not change with β. This approximation can be applied either when β is small enough, or when both materials are very similar and the effective masses differ only by a few percent. We will denote the solutions for different R and β by

$$E_\lambda(R,\beta), \quad \Psi_{\lambda,R,\beta}(\mathbf{r}).$$

We add the index R to describe the dependence of the effective mass (4) and of the potential (5) on the dot radius. Let us notice that both $U_R(\mathbf{r})$ and $\mu_R(\mathbf{r})$ can be rewritten as functions of $\mathbf{x}=\mathbf{r}/R$; for example,

$$U_R(\mathbf{r})=u(\mathbf{x})=\begin{cases} -U_0, & |x|<1 \\ 0, & |x|\geqslant 1. \end{cases} \tag{A1}$$

As a consequence, Eq. (3) can be given in the form

$$\left[-\nabla_x \frac{1}{\mu(\mathbf{x})}\nabla_x + R^2\beta u(\mathbf{x})\right]\Psi_{\lambda R,\beta}(\mathbf{x}\cdot\mathbf{R}) = R^2 E_\lambda(R,\beta)\Psi_{\lambda,R,\beta}(\mathbf{x}\cdot\mathbf{R}). \tag{A2}$$

It is easy to see that the operator inside the square brackets will not change on replacing $\mathbf{R}$ by $\sqrt{\beta}\mathbf{R}$ and β by 1. The equation (A2) becomes then

$$\left[-\nabla_x \frac{1}{\mu(\mathbf{x})}\nabla_x + \beta R^2 u(\mathbf{x})\right]\Psi_{\lambda,\sqrt{\beta}R,1}(\mathbf{x}\cdot\sqrt{\beta}\mathbf{R}) = \beta R^2 E_\lambda(\sqrt{\beta}R,1)\Psi_{\lambda,\sqrt{\beta}R,1}(\mathbf{x}\cdot\sqrt{\beta}\mathbf{R}). \tag{A3}$$

Hence the solutions can be scaled so that

$$E_\lambda(R,\beta)=\beta E_\lambda(\sqrt{\beta}R,1),$$

and

$$\Psi_{\lambda,R,\beta}(\mathbf{r})=C\Psi_{\lambda,\sqrt{\beta}R,1}(\sqrt{\beta}\mathbf{r}). \tag{A4}$$

The value of the coefficient C is given by the normalization condition for the wave function. If we normalize to 1 for the discrete spectrum and to $\delta(E-E_\lambda)$ for the continuum, we obtain $C=\beta^{3/4}$ and $C=\beta^{1/4}$, respectively.

The equations (A4) allow one to scale the matrix elements of any operator. For example, the scaling of the oscillator strengths is given by

$$f_{0,n}(R,\beta)=f_{0,n}(\sqrt{\beta}R,1) \quad \text{(discrete states)},$$

$$f_{0,E}(R,\beta)=\frac{1}{\beta}f_{0,(1/\beta)E}(\sqrt{\beta}R,1) \quad \text{(continuum spectrum)}. \tag{A5}$$

It is worth noticing that the scaling theorem (A4) and (A5) can be extended to any other quantum structure with reduced

dimensionality, when the structure diameter can be parametrized by a single variable. The parameter R (the radius of the quantum dot) can be, for example, replaced by the radius of the cross section of a quantum wire or by the width of a quantum well. Finally, we notice that the scaling procedure allows us to obtain results not only by considering the increase of the potential but also by homogeneous enlargement of the size of the structure.

[1] See, for example, A. D. Yoffe, Adv. Phys. **42**, 173 (1993), and references therein.

[2] J. Cibert, P. M. Petrov, G. J. Dolan, S. J. Pearton, A. C. Gossard, and J. H. English, Appl. Phys. Lett. **49**, 1043 (1986).

[3] A. I. Ekimov, Al. L. Efros, and A. A. Onushchenko, Solid State Commun. **56**, 921 (1985).

[4] N. F. Borrelli, D. W. Hall, H. J. Holland, and D. W. Smith, J. Appl. Phys. **61**, 5399 (1987).

[5] Jian-Bai Xia, Phys. Rev. B **40**, 8500 (1989).

[6] P. C. Sercel and K. J. Vahala, Phys. Rev. B **42**, 3690 (1990).

[7] M. Wagner, U. Merkt, and A. V. Chaplik, Phys. Rev. B **45**, 1951 (1992).

[8] J. Tulkki and A. Henämäki, Phys. Rev. B **52**, 8239 (1995).

[9] Jia-Lin Zhu, Jie-Hua Zhao, and Jia-Jiong Xiong, Phys. Rev. B **50**, 1832 (1994).

[10] J.-Y. Marzin and G. Bastard, Solid State Commun. **92**, 437 (1994).

[11] D. S. Chuu, C. M. Hsiao, and W. N. Mei, Phys. Rev. B **46**, 3898 (1992).

[12] Jia-Lin Zhu, Jia-Jiong Xiong, and Bing-Lin Gu, Phys. Rev. B **41**, 6001 (1990).

[13] Zhen-Yan Deng, Jing-Kun Guo, and Ting-Rong Lai, Phys. Rev. B **50**, 5736 (1994).

[14] N. Porras-Montenegro, S. T. Pérez-Merchancano, and A. Latgé, J. Appl. Phys. **74**, 7624 (1993).

[15] Jia-Lin Zhu and Xi Chen, Phys. Rev. B **50**, 4497 (1994).

[16] E. Wigner, Phys. Rev. **98**, 145 (1955); G. Breit, *ibid.* **107**, 1612 (1957).

[17] See, for example, R. G. Newton, *Scattering Theory of Waves and Particles* (McGraw-Hill, New York, 1966).

[18] U. Fano, Phys. Rev. **124**, 1866 (1961); U. Fano and J. W. Cooper, Rev. Mod. Phys. **40**, 441 (1968).

[19] L. E. Brus, J. Chem. Phys. **80**, 4403 (1984).

[20] L. Banyai, P. Gilliot, Y. Z. Hu, and S. W. Koch, Phys. Rev. B **45**, 14 136 (1991).

[21] D. B. Tran Troai, Solid State Commun. **85**, 39 (1993).

[22] D. Babić, R. Tsu, and R. F. Greene, Phys. Rev. B **45**, 14 150 (1992).

[23] See, for example, C. J. Joachain, *Quantum Collision Theory* (North-Holland, Amsterdam, 1975), Sec. 4.5.

[24] W. Magnus, F. Oberhettinger, and R. P. Soni, *Formulas and Theorems for the Special Functions of Mathematical Physics* (Springer-Verlag, Berlin, 1966).

[25] M. Born and E. Wolf, *Principles of Optics*, 6th ed. (Pergamon, Oxford, 1986), Chap. XIII.

[26] D. P. Davé and H. F. Taylor, Phys. Lett. A **184**, 301 (1994).

[27] V. Milanovic and Z. Ikonic, Phys. Rev. B **39**, 7982 (1988).

[28] B. El Jani, P. Gibart, J. C. Portal, and R. L. Aulombard, J. Appl. Phys. **58**, 3481 (1985).

[29] *Semiconductors. Physics of Group IV Elements and III-V Compounds*, edited by O. Madelung, M. Schultz, and H. Weiss, Landolt-Börnstein, New Series, Group III, Vol. 17, Pt. a (Springer-Verlag, Berlin, 1982); *Semiconductors. Intrinsic Properties of Group IV Elements and III-V, II-VI, and I-VII Compounds*, edited by O. Madelung, Landolt-Börnstein, New Series, Group III, Vol. 22, Pt. a (Springer-Verlag, Berlin, 1987); S. Adachi, J. Appl. Phys. **58**, R1 (1985).

[30] J. M. Langer, Ch. Delerue, M. Lannoo, and H. Hennrich, Phys. Rev. B **11**, 7723 (1988).